Extended Klein Edges in Graphene

Kuang He,[†] Alex. W. Robertson,[†] Sungwoo Lee,[‡] Euijoon Yoon,[‡] Gun-Do Lee,[‡] and Jamie H. Warner*[,†]

[†]Department of Materials, University of Oxford, Parks Road, Oxford OX1 3PH, United Kingdom and [‡]Department of Materials Science and Engineering, Seoul National University, Seoul 151-742, Republic of Korea

ABSTRACT Graphene has three experimentally confirmed periodic edge terminations, zigzag, reconstructed 5−7, and arm-chair. Theory predicts a fourth periodic edge of graphene called the extended Klein (EK) edge, which consists of a series of single C atoms protruding from a zigzag edge. Here, we confirm the existence of EK edges in both graphene nanoribbons and on the edge of bulk graphene using atomic resolution imaging by aberration-corrected transmission electron microscopy. The formation of the EK edge stems from sputtering and reconstruction of the zigzag edge. Density functional theory reveals minimal energy for EK edge reconstruction and bond distortion both in and out of plane, supporting our TEM observations. The EK edge can now be included as the fourth member of observed periodic edge structures in graphene.

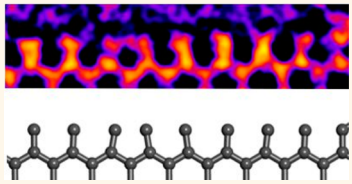

KEYWORDS: graphene · TEM · Klein edge · aberration-correction

The properties of graphene, especially nanoribbons, are influenced by the edge's atomic structure.[1−7] So far three classifications of periodic graphene edge terminations have been experimentally confirmed: the zigzag, reconstructed zigzag (rec5−7), and armchair edges.[8−17] However, a fourth type of periodic edge structure has been theoretically predicted, consisting of an array of single carbon atoms extending from a zigzag edge, which can be described as an extended Klein (EK) edge,[18,19] but has never been experimentally observed or verified beyond the single Klein edge level. It has been assumed that arrays of dangling carbon atoms at the edges of graphene would be unstable, limiting previous studies to artificial "photonic graphene".[20] To experimentally confirm the predicted EK edge with convincing evidence, it is important to directly image the atomic structure.

Aberration-corrected transmission electron microscopy (AC-TEM) has proven to be an excellent method for studying the atomic structure of graphene.[21,22] Using low accelerating voltages (80 kV and below) in AC-TEM has permitted the study of defects, dopants, edges and layer stacking sequences at the atomic level.[13,23,24] Studies of graphene edges show that zigzag, armchair, and rec5−7 form long-range periodic terminations,[12,14] while at the shorter scale, other unusual structures can form, such as carbon chains and the single atom Klein edge.[9,25] Real-time AC-TEM image sequences of graphene edges have shown interesting atomic scale dynamics such as migration of C atoms along the edges, single atom sputtering from graphene edges, bond rotations, and the rapid switching of zigzag edges to rec5−7 edges.[11] Scanning AC-TEM (AC-STEM) combined with atomic resolution electron energy loss spectroscopy (EELS) has confirmed that energy states of carbon atoms at the edge of graphene are different to those in bulk graphene.[9,26]

Monochromation of the electron source in an aberration-corrected TEM has been demonstrated to improve the spatial resolution such that the position of individual C atoms in graphene can be resolved and consequently precise C−C bond lengths to be measured.[10,16,27−29] This enabled the first correlations at the single atom level between bond length changes and electron charge density variations within vacancy defects in graphene.[21,30] Recent work extended this to armchair edges in graphene to reveal significant bond contract and confirm the existence of hydrogen-free graphene edges.[13] In this report, we use the improvement in spatial resolution achieved by monochromation of the electron source in AC-TEM, operating at an accelerating voltage of 80 kV, to accurately identify EK edges in graphene and nanoribbon structures. Monolayer graphene samples were prepared using chemical vapor deposition (CVD) on liquid copper and were transferred onto silicon nitride TEM grids with 2-μm holes.[31,32]

* Address correspondence to Jamie.Warner@materials.ox.ac.uk.

Received for review August 11, 2014 and accepted November 18, 2014.

Published online November 25, 2014
10.1021/nn504471m

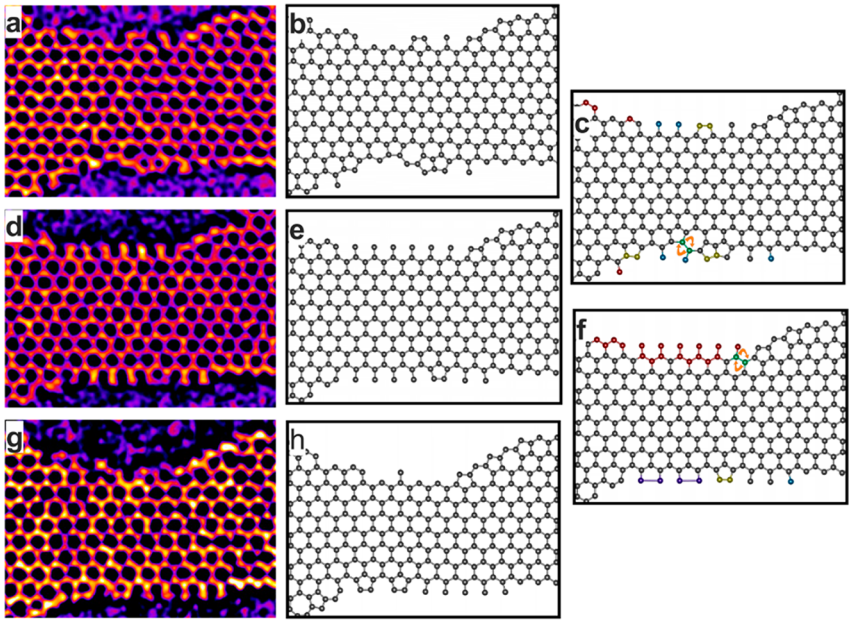

Figure 1. Dynamics of extended Klein edges in a graphene nanoribbon. (a, d, and g) Three consecutive AC-TEM frames remarking on the appearance of double sided multiple Klein edges and the frames prior and after it. The raw AC-TEM images are shown in Supporting Information Figure S2 and the image processing techniques are shown in Supporting Information Figure S3. (b, e, and h) The corresponding atomistic model of (a, d, g). Panels c and f describe the transition from (b) to (e) and (e) to (h), respectively. The atoms on the edge are highlighted with different colors to remark on the different transition different atoms underwent. Red indicates atom loss, blue indicates atom addition, green indicates near edge stone-wales rotation, the arrows around the green atoms indicate the direction of stone-wales rotation, and yellow indicates bond breakage and purple indicates bond reconstruction.

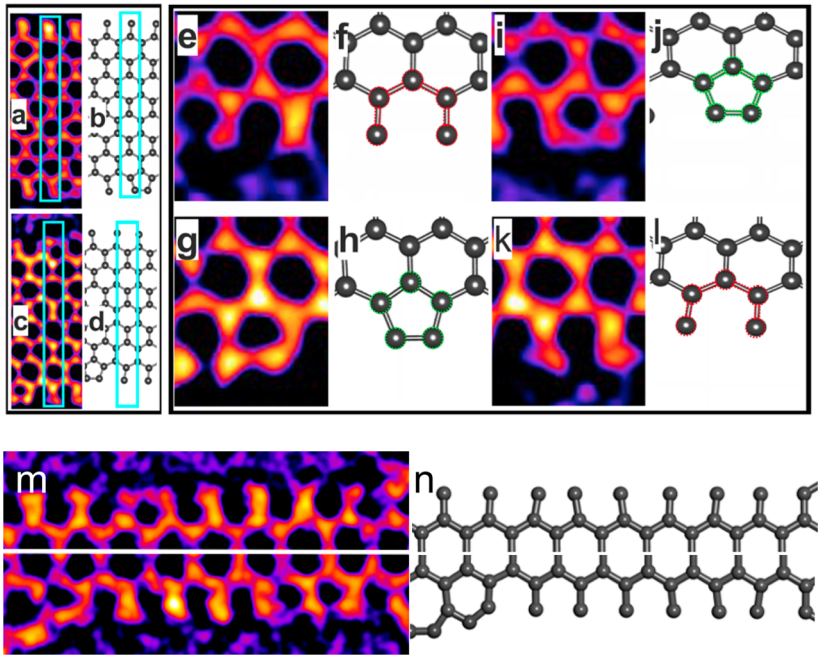

Figure 2. Detailed analysis of extended Klein edge symmetry in a graphene nanoribbon. (a and b) AC-TEM and the atomistic model of a symmetric EK edge. (c and d) AC-TEM and the atomistic model of an offset EK edge. Panels e–h demonstrate the mechanism of multiple Klein edges' reconstruction; panels e and f demonstrate the AC-TEM image and atomistic model of multiple Klein edges' in their unreconstructed states; and panels g and h illustrate the reconstructed structure. Panels i–l demonstrate the dereconstructing procedure, with (i) and (j) being the initial structure, and (k) and (l) being the subsequent structure. (m) AC-TEM image of the two sides of the EK GNR with corresponding atomic models in (n).

RESULTS AND DISCUSSION

The graphene nanoribbon (GNR ~15 nm wide) in Figure 1 was formed by sputtering two holes into a pristine sheet using 80 kV electron irradiation (Supporting Information Figure S1). The GNR runs parallel to the zigzag lattice direction and in Figure 1a the

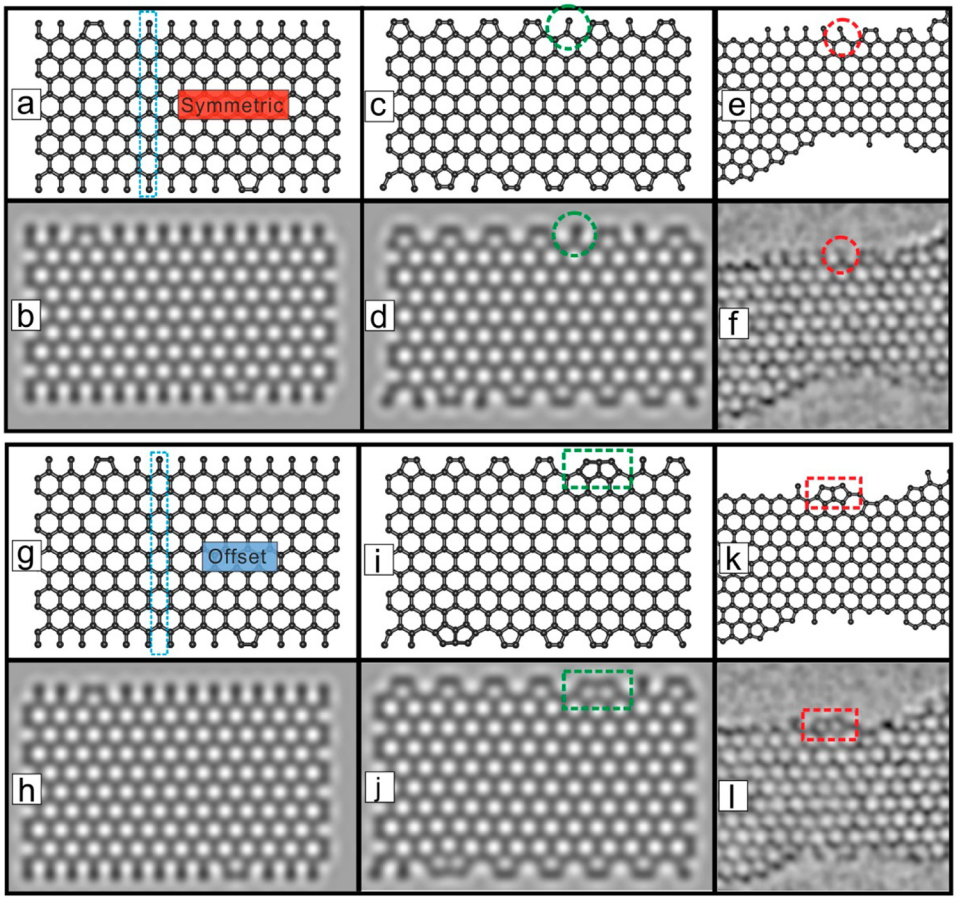

Figure 3. (a and c) The atomistic models of the initial and fully relaxed structures in DFT calculation of symmetric EK edges on a graphene nanoribbon; (b and d) the multislice image simulations of the structures, respectively. TEM image shown in (f) and its model (e) illustrate the same reconstruction and Klein edge bending effect as observed in the DFT calculation. (g−l) The same analysis applied to an offset EK edge on a graphene nanoribbon.

edges generally appear in zigzag form with distortions from pentagons, heptagons and the occasional single Klein atom. Seconds later (Figure 1d), the edge has transformed to form EK edges on both sides of the GNR. This double GNR EK edge was stable for 2 s during image acquisition before undergoing further structural transformations (Figure 1g). The structural transformations, Figure 1c,f, occur through a combination of atom loss, bond breakage and reformation, and Stone−Wales bond rotation.[33] To our knowledge, this is the first experimental observation of an EK edge in graphene as well as a double-sided EK edge structure in a GNR. Prior work on imaging extended Klein edge structures has been limited to 2−3 atom sequences.[9,10]

A double EK edge in a GNR can have the EK edges on either side be symmetric or offset by one atomic row (Supporting Information Figure S4). A detailed analysis of the double EK edge structure from Figures 1b and 2a,b shows a symmetric EK edge for the GNR. After the GNR undergoes structural transformation, as shown in Figure 1g, a row of EK edge atoms are lost and this results in breaking of the symmetry and the resultant offset between the top and bottom EK edges, Figure 2c,d. Occasionally, pairs of atoms within an EK edge rebond to form 5-membered rings at the edge, Figure 2e−h. The reverse process also occurs, where the bond breaks between the two outermost atoms in a 5-membered ring at the edge to form two single Klein edges. The reconstruction and dereconstruction of bonding took place over the time period of 1 frame (∼15 s), and is driven by energy supplied from the electron beam. These sequences not only demonstrate the dynamic loss and addition of atoms at the edges, but also the occurrence of frequent bond breakage and reconstruction. Examination of the two sides of the EK edge in the GNR from Figures 1d and 2m,n reveals that some atoms along the EK edge deviate in angle from the 120° sp^2 bonding.

To understand reconstruction processes of the EK edges, we have performed density functional theory (DFT) calculation on both symmetric and offset EK edges. In Figure 3a, two single Klein edges are initially bonded to form a 5 membered ring (pentagon) on both sides of a symmetric EK edge; Figure 3b shows the AC-TEM image simulation. When the structure is relaxed by DFT calculation, a majority of the EK edges also reconstruct to form pentagonal edge terminations, Figure 3c, with the AC-TEM image simulation in

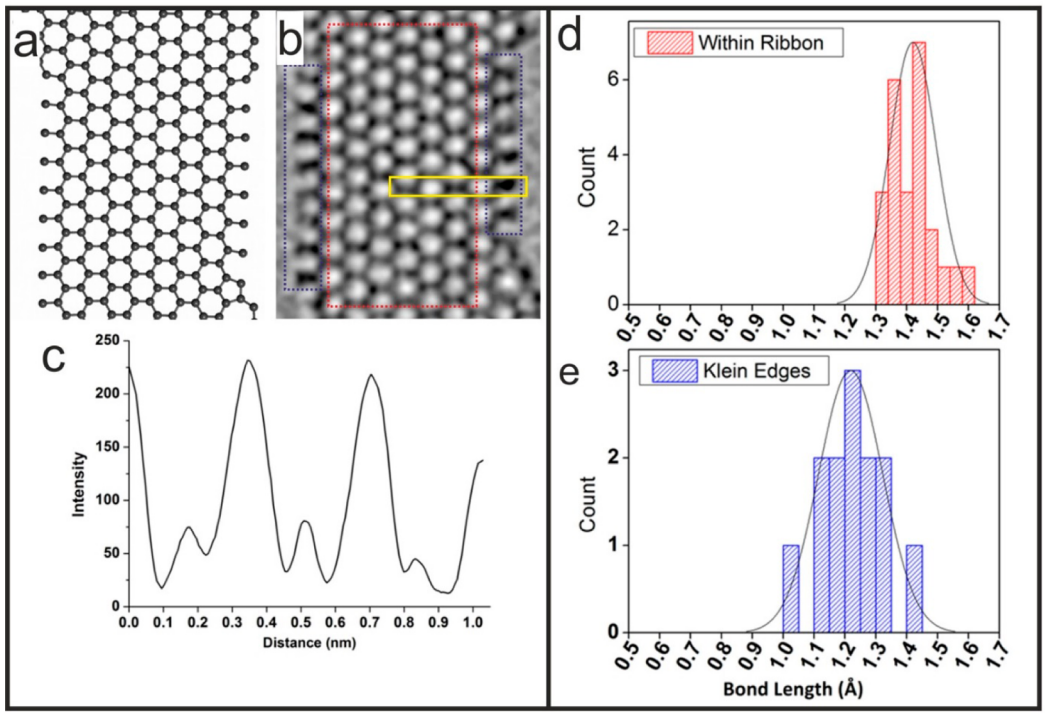

Figure 4. EK edge bond length analysis. (a) Schematic atomic model to demonstrate the structure imaged in (b). (b) AC-TEM image of a double EK edge graphene nanoribbon. (c). A typical intensity *vs* distance profile taken from the yellow box region in (b). (d) Histogram of the bond length distribution within the graphene nanoribbon as indicated by the red box in (b). (e) Histogram of the bond length distribution of the Klein edges, taken within the region of blue box in (b).

Figure 3d. Not all the Klein edges have reconstructed, with the green dashed circle in Figure 3c showing a single Klein edge remaining, but with deviation from a pristine perpendicular orientation. We have observed several cases in our experimental AC-TEM images where single Klein edges next to pentagonal edge terminations have nonperpendicular orientation, with an example shown in Figure 3e,f. The structural relaxations for the offset EK edges in a graphene nanoribbon are shown in Figure 3g–j. The major difference observed compared to the symmetric EK edges is that a double pentagon edge termination arises, Figure 3i,j. We have experimentally observed this double pentagon structure, Figure 3k,l.

It is interesting to note that the positions of the double pentagon structures observed in Figure 3i coincide with the location directly opposite to the original position of the pentagon formation in Figure 3g. Likewise in the symmetric EK edge case, we can see that the two bent single Klein edges in Figure 3c are formed directly opposite to the location of the two original pentagons in Figure 3a. This indicates that there is some cross talk between bonding events that happen on one side of the nanoribbon with the other side. This might be related to some strain induced effects caused by bond restructuring within the nanoribbons. The reason that we do not see extended pentagonal ring edge terminations in our experimental TEM images is because the edges are being continuously sputtered by the removal of atoms. This has the effect of disrupting the long-range periodicity required to transition from the EK edges to the reconstructed pentagonal edge arrays. The sputtering of the EK edge will turn it back to a zigzag edge structure, as we shall see later in Figure 6. However, Figure 2 along with Figure 3f,l, show that within an EK edge bond reconstruction can occur, leading to the formation of pentagonal edge structures.

The details of the EK edges can be further analyzed by measuring changes to the bond lengths both within the ribbon and on the EK edges. In the AC-TEM image of Figure 4b, the C–C bond lengths were determined by fitting double Gaussian peaks to the intensity profiles for each pair of atoms forming a bond. A typical box profile is taken from the yellow boxed region of Figure 4b and is shown in Figure 4c. The distribution of bond lengths within the ribbon (marked by red box in Figure 4b) and on the Klein edges (marked by blue boxes) are shown in Figure 4, panels d and e, respectively. The distributions were then fitted with a normal distribution equation, the peak position of the "within ribbon" bond lengths is set to 1.42 Å, and as a result, the peak position of the "Klein edges" bond lengths is measured at 1.24 Å. These values represent the average C–C bond lengths within these regions.

We have also employed DFT to relax pristine and hydrogenated EK edge structures, as shown in Supporting Information Figure S5. The calculated bond length of nonfunctionalized EK edges and hydrogen functionalized EK edges are 1.38 and 1.36 Å,

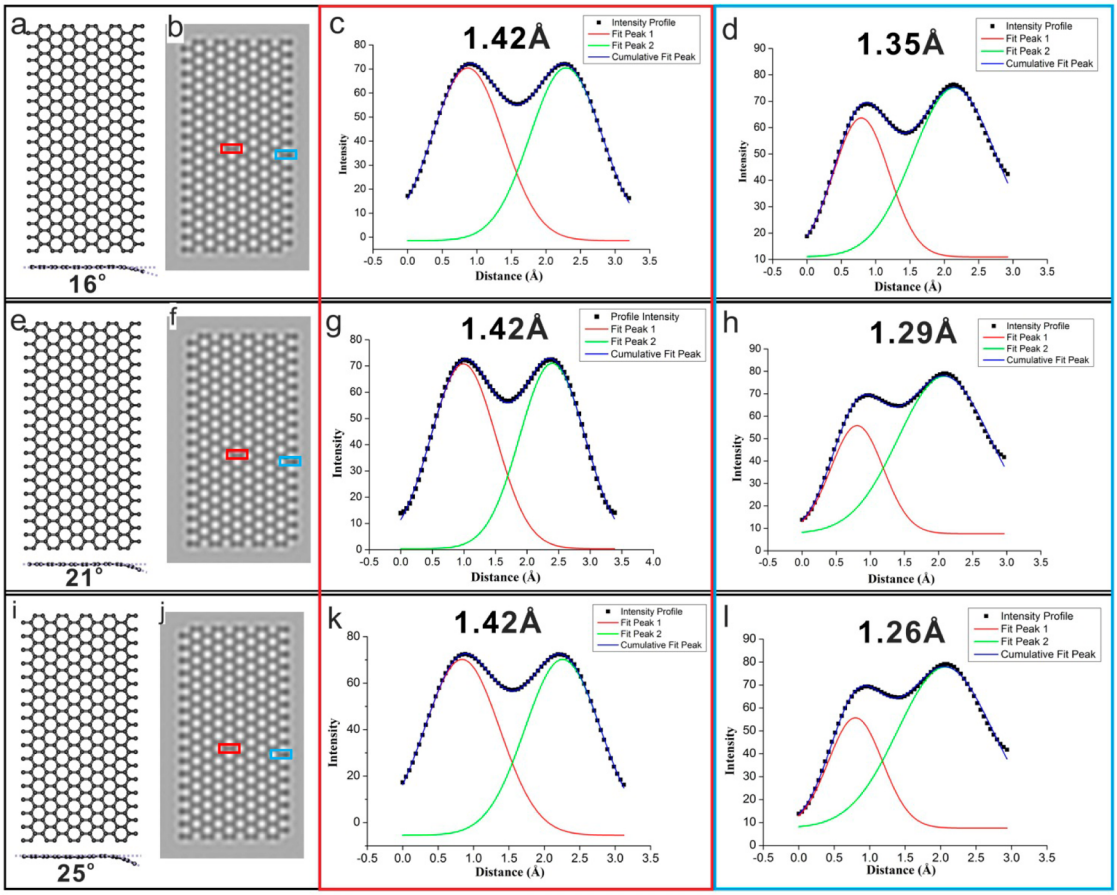

Figure 5. Density functional theory calculations of bent EK edges. One side of the graphene nanoribbon with EK edge is bent 16° out of plane as shown in the front and side view of the atomic model in (a) with its multislice image simulation shown in (b). The box profiles taken from the red and blue boxed region of (b) are shown in (c) and (d), respectively; the intensity profiles are fitted by two Gaussian curves to measure the bond length. (e−h) and (i−l) The same analysis applied to 21° and 25° bent nanoribbon structures.

respectively. The average experimentally observed bond length for EK edges is 1.24 Å as shown in Figure 4e. This bond length value is significantly shorter than both pristine and hydrogenated EK edges. To understand this difference we have examined the possibility of out-of-plane distortions for the EK edges arising from bending of the GNRs. Each repeating unit shown in Supporting Information Figure S6 was bent out of plane to different angles, and then relaxed by DFT. This unit structure was then laterally extended to form a nanoribbon structure to simulate the bent EK edge scenario. As shown in Figure 5, three different amounts of bending distortion are explored; 16°, 21°, and 25°. The intensity profiles in the center of the ribbon (red rectangle regions in Figure 5b,f,j are fitted with two Gaussian curves and the separation between the two peak positions are set to 1.42 Å from the simulated atomic model. The intensity profiles taken from the blue rectangle region of Figure 5b,f,j are fitted by two Gaussian curves as well to determine the bond length of the EK edges by measuring the peak separation, the results are shown in Figure 5d,h,l. The bond lengths measured from the simulated HRTEM images are 1.35, 1.29, and 1.26 Å for the 16°, 21°, and 25° bent structures. The energy of the repeating unit for structures in Figure 5a,e,l are only 0.19, 0.39, and 0.53 eV higher than the pristine in plane model shown in Supporting Information Figure S5a, well below the maximum energy that can be transferred by an 80 keV electron to a carbon atom.[34] It is therefore plausible to suggest some EK edges might have suffered different degrees of bending to allow the bond length appear shorter in TEM image compare to its intrinsic bond length.

We also observed EK structures at the edges of bulk graphene, Figure 6. Time dependent imaging, Figure 6a,d,g,j, shows a section of an atomically defined zigzag edge losing six of the outermost atoms, Figure 6c, resulting in the formation of the EK edge, Figure 6d. Further atoms are then sputtered, Figure 6d−k, leading to the reformation of the zigzag edge. This sequence of images provide insights into the process of electron beam sputtering for zigzag edges, whereby the edge can alternate between zigzag and EK, as carbon atoms are sequentially lost. The transition process between these stable zigzag or

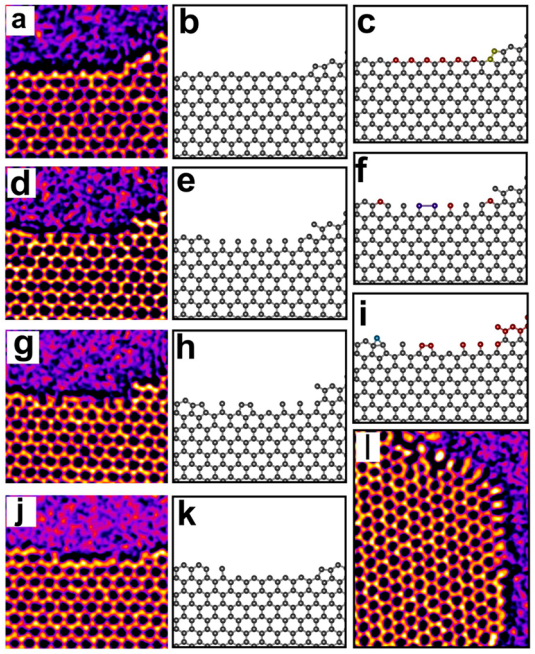

Figure 6. Formation of extended Klein edges from zigzag edges in graphene. (a, d, g, and j) Four consecutive TEM frame of the appearance and transformation of multiple Klein edge on the edge of bulk graphene. The raw TEM images are shown in Supporting Information Figure S5. (b, e, h, and k) The atomistic model describing the crystal structure of the TEM image on its left-hand side. (c, f, and i) Atomistic model with edge atoms remarked with different colors to illustrate different transformation those edge atoms underwent. Red indicates atom loss, blue indicates atom addition, yellow indicates bond breakage, and purple indicates bond reconstruction. (l) Observation of extra-long EK edge over a curved edge.

EK configurations involves bond breakage, atom loss, bond reformation, as in the case of the GNR in Figure 1. We have also observed EK edges deviating from pure linear edge form, and extending throughout a change in lattice direction, Figure 6l. A total number of 10 individual Klein atoms are identified in this case as it curve around the edge to follow the landscape of the structure.

Edges of graphene observed during AC-TEM are those which are stable against electron beam irradiation, and do not necessarily represent the thermodynamics. Recent DFT calculations have explored the displacement thresholds for nearly all known graphene edge types.[35] Armchair edges were calculated to have the highest displacement threshold, meaning they are the most radiation stable edge, and this explains why they are the most abundant edge type observed in graphene.[35] Surprisingly, the DFT calculations showed that Klein edges have a higher displacement threshold and consequently higher radiation stability than zigzag edges.[35] The low radiation stability of zigzag edges is related to the limited flexibility of its edge atoms. Given the theoretical calculations in ref 35, it is not unexpected to see highly stable extended Klein edges in graphene, and we believe that the reason many of these structures were not previously observed is due to the challenges in identifying them from zigzag edges.

CONCLUSION

Our success has been helped by improvements in the spatial resolution of our AC-TEM by monochromation of the electron source to reduce the effects of chromatic aberration.[20] The EK edges are difficult to identify when spatial resolution is not improved by addressing detrimental chromatic aberration effects. Extra AC-TEM images taken without monochromation of the electron source are shown in Supporting Information Figure S8 and demonstrate that EK edges are not easy to identify in AC-TEM images. The EK edges form as part of the sputtering process of zigzag edges and remain for several seconds, before being further sputtered back to zigzag form. Not only have we verified the existence of a fourth periodic edge structure of graphene, but we have also confirmed that symmetric double EK edges can form on GNRs.

METHODS

CVD Growth of Graphene on Liquid Copper. The graphene used in this experiment was synthesized by atmospheric pressure CVD, the complete details of which can be found in ref 29. Copper foil (Alfa Aesar, puratonic 99.999% purity, 0.1 mm thick) of ~1 cm^2 was used as a catalyst, resting on top of a similar-sized piece of molybdenum (Alfa Aesar, 99.95% purity, 0.1 mm thick). This was loaded into the quartz tube of the split-tube furnace CVD system, which was subsequently sealed and tested with a vacuum pump. The tube was then flushed with 200 sccm Ar, 100 sccm H_2/Ar mix (25% H_2) and 100 sccm CH_4/Ar mix (1% CH_4) gas flow for 30 min at room temperature. The catalyst was then subjected to a 30 min anneal at 1100 °C under 200 sccm Ar and 100 sccm H_2/Ar mix gas flow, melting the copper. The H_2/Ar mix flow was reduced to 80 sccm and the CH_4/Ar mix was set enabled at 10 sccm for 90 min at the same temperature. Following this, the sample was removed from the heating region of the furnace and rapidly cooled at ambient temperature under a H_2 and Ar atmosphere.

Transfer onto TEM Grid. A (8 wt % in anisole, 495 molecular weight) PMMA was spin coated onto the graphene side of the sample at 4500 rpm for 60 s, and then cured at 180 °C for 90 s. The underlying molybdenum and copper were etched away by floating the sample on iron(III) chloride and hydrochloric acid solution for 3 days, until just a transparent PMMA/graphene film remained suspended on the surface. This was then cleaned by floating onto fresh DI water and 30% hydrochloric acid, respectively, and then cleaned in DI water again. The film was then transferred to a holey silicon nitride TEM grid (Agar Scientific). Once left to dry for about 3 h, the sample was baked on a hot plate for 15 min to remove water and improve sample adhesion with the TEM grid. The sample was then placed in a furnace at 350 °C overnight to remove the PMMA scaffold.

High Resolution Transmission Electron Microscopy. HRTEM imaging was performed using the Oxford-JEOL JEM 2200MCO field-emission gun transmission electron microscope, fitted with CEOS probe and image aberration correctors and a double Wien Filter monochromator operated with a 5 μm slit to reduce

the energy spread of the electron beam to 217 meV at an accelerating voltage of 80 kV. Images were recorded using a Gatan Ultrascan 4k × 4k CCD camera with 2 s acquisition times. The sample height was continuously adjusted by a piezo controller to maintain a defocus value of ~1 nm. Edges were created in graphene using a focused electron beam with beam current density (BCD) of $\sim 1 \times 10^8$ e s^{-1} nm^{-2} with 5 min exposure time. Once a small hole was created, the beam is expanded to a reduced BCD of $\sim(0.1-1) \times 10^6$ e s^{-1} nm^{-2} and images are acquired.

Image Processing. Image processing was performed in ImageJ software. First, a FFT band-pass filter between 100 to 1 pixels was used to remove the broad uneven illumination variation, and the image was then smoothed to remove further noise. A color look-up table (LUT) "Fire" in ImageJ software was used to improve visual contrast. Great care was taken to ensure these processes do not introduce artifacts in the final images. Multislice image simulations were performed using JEMS software with supercells. The supercell structures were created using Accelrys Discovery Studio Visualizer.

Density Functional Theory (DFT) Calculations. The DFT total energy calculations were performed to understand reconstruction processes of the EK edges and to relax pristine and hydrogenated EK edge structures. The DFT calculations are performed within the generalized gradient approximation of Perdew–Burke–Ernzerhof (PBE) functional[36] using Vienna *ab initio* simulation package (VASP) code.[37] The basis set contains plane waves up to an energy cutoff of 400 eV. The supercells in our simulations contain 252 atoms for the symmetric EK edge GNR and 280 atoms for the offset EK edge GNR, and 20 atoms for the calculation of bending edge shown in Figure 5a,e,i. In constructing the super cell for simulation, we contain a vacuum region of 30 Å in the *y* and *z* direction. The Brillouin zone was sampled using a (2 × 2 × 1) Γ-centered mesh for the symmetric and offset EK edge GNR and a (12 × 2 × 1) Γ-centered mesh for the calculation of bending edge. In the structural relaxations, the structures are fully relaxed until the force is smaller than 0.02 eV/Å except the calculation of bending edges in which the structures are relaxed under the constraint keeping the bending.

Conflict of Interest: The authors declare no competing financial interest.

Acknowledgment. J.H.W thanks the Royal Society for support. G.-D.L. and E.Y. acknowledge support from the Supercomputing Center/Korea Institute of Science and Technology Information with supercomputing resources (KSC-2014-C3-009), from BK21 plus program, and from the National Research Foundation of Korea (NRF) grant funded by the Korea Government (RIAM No. 2010-0012670, MSIP No. 20080061900).

Supporting Information Available: Supplementary figures showing the fabrication process of GNRs, raw TEM images, image processing techniques employed, display of symmetric and offset EK edge model, DFT calculation of pristine and hydrogenated EK edges, and nonmonochromation TEM images of EK edges. This material is available free of charge *via* the Internet at http://pubs.acs.org.

REFERENCES AND NOTES

1. Ritter, K. A.; Lyding, J. W. The Influence of Edge Structure on the Electronic Properties of Graphene Quantum Dots and Nanoribbons. *Nat. Mater.* **2009**, *8*, 235–242.
2. Son, Y.-W.; Cohen, M. L.; Louie, S. G. Half-Metallic Graphene Nanoribbons. *Nature* **2006**, *444*, 347–349.
3. Chen, Z.; Lin, Y.-M.; Rooks, M. J.; Avouris, P. Graphene Nano-Ribbon Electronics. *Phys. E* **2007**, *40*, 228–232.
4. Son, Y.-W.; Cohen, M. L.; Louie, S. G. Energy Gaps in Graphene Nanoribbons. *Phys. Rev. Lett.* **2006**, *97*, 216803.
5. Han, M.; Özyilmaz, B.; Zhang, Y.; Kim, P. Energy Band-Gap Engineering of Graphene Nanoribbons. *Phys. Rev. Lett.* **2007**, *98*, 206805.
6. Akhmerov, a.; Beenakker, C. Boundary Conditions for Dirac Fermions on a Terminated Honeycomb Lattice. *Phys. Rev. B* **2008**, *77*, 085423.
7. Kunstmann, J.; Özdoğan, C.; Quandt, A.; Fehske, H. Stability of Edge States and Edge Magnetism in Graphene Nanoribbons. *Phys. Rev. B* **2011**, *83*, 045414.
8. Koskinen, P.; Malola, S.; Häkkinen, H. Self-Passivating Edge Reconstructions of Graphene. *Phys. Rev. Lett.* **2008**, *101*, 115502.
9. Suenaga, K.; Koshino, M. Atom-by-Atom Spectroscopy at Graphene Edge. *Nature* **2010**, *468*, 1088–1090.
10. Liu, Z.; Suenaga, K.; Harris, P.; Iijima, S. Open and Closed Edges of Graphene Layers. *Phys. Rev. Lett.* **2009**, *102*, 015501.
11. Girit, Ç. Ö.; Meyer, J. C.; Erni, R.; Rossell, M. D.; Kisielowski, C.; Yang, Li; Park, C.-H.; Crommie, M. F.; Cohen, M. L.; Louie, S. G.; Zetti, A. Graphene at the Edge: Stability and Dynamics. *Science* **2009**, *666*, 1705–1708.
12. Koskinen, P.; Malola, S.; Häkkinen, H. Evidence for Graphene Edges beyond Zigzag and Armchair. *Phys. Rev. B* **2009**, *80*, 073401.
13. He, K.; Lee, G.-D.; Robertson, A. W.; Yoon, E.; Warner, J. H. Hydrogen-Free Graphene Edges. *Nat. Commun.* **2014**, *5*, 3040.
14. Kim, K.; Coh, S.; Kisielowski, C.; Crommie, M. F.; Louie, S. G.; Cohen, M. L.; Zettl, A. Atomically Perfect Torn Graphene Edges and Their Reversible Reconstruction. *Nat. Commun.* **2013**, *4*, 2723.
15. Westenfelder, B.; Meyer, J. C.; Biskupek, J.; Kurasch, S.; Scholz, F.; Krill, C. E.; Kaiser, U. Transformations of Carbon Adsorbates on Graphene Substrates under Extreme Heat. *Nano Lett.* **2011**, *11*, 5123–5127.
16. Meyer, J. C.; Kisielowski, C.; Erni, R.; Rossell, M. D.; Crommie, M. F.; Zettl, A. Direct Imaging of Lattice Atoms and Topological Defects in Graphene Membranes. *Nano Lett.* **2008**, *8*, 3582–3586.
17. Lee, G.-D.; Wang, C. Z.; Yoon, E.; Hwang, N.-M.; Ho, K. M. Reconstruction and Evaporation at Graphene Nanoribbon Edges. *Phys. Rev. B* **2010**, *81*, 195419.
18. Klein, D. J. Graphitic Polymer Strips with Edge States. *Chem. Phys. Lett.* **1994**, *217*, 261–265.
19. Klein, D. J.; Bytautas, L. Graphitic Edges and Unpaired Π-Electron Spins. *J. Phys. Chem. A* **1999**, *103*, 5196–5210.
20. Plotnik, Y.; Rechtsman, M. C.; Song, D.; Heinrich, M.; Zeuner, J. M.; Nolte, S.; Lumer, Y.; Malkova, N.; Xu, J.; Szameit, A.; *et al.* Observation of Unconventional Edge States in "Photonic Graphene". *Nat. Mater.* **2014**, *13*, 57–62.
21. Warner, J. H.; Margine, E. R.; Mukai, M.; Robertson, A. W.; Giustino, F.; Kirkland, A. I. Dislocation-Driven Deformations in Graphene. *Science* **2012**, *337*, 209–212.
22. Warner, J. H.; Lee, G.-D.; He, K.; Robertson, A. W.; Yoon, E.; Kirkland, A. I. Bond Length and Charge Density Variations within Extended Arm Chair Defects in Graphene. *ACS Nano* **2013**, *7*, 9860–9866.
23. Warner, J. H.; Liu, Z.; He, K.; Robertson, A. W.; Suenaga, K. Sensitivity of Graphene Edge States to Surface Adatom Interactions. *Nano Lett.* **2013**, *13*, 4820–4826.
24. Robertson, A. W.; He, K.; Kirkland, A. I.; Warner, J. H. Inflating Graphene with Atomic Scale Blisters. *Nano Lett.* **2014**, *14*, 908–914.
25. Chuvilin, A.; Meyer, J. C.; Algara-Siller, G.; Kaiser, U. From Graphene Constrictions to Single Carbon Chains. *New J. Phys.* **2009**, *11*, 083019.
26. Warner, J. H.; Lin, Y.; He, K.; Koshino, M.; Suenaga, K. Atomic Level Spatial Variations of Energy States along Graphene Edges. *Nano Lett.* **2014**, *14*, 6155–6159.
27. Kabius, B.; Hartel, P.; Haider, M.; Müller, H.; Uhlemann, S.; Loebau, U.; Zach, J.; Rose, H. First Application of Cc-Corrected Imaging for High-Resolution and Energy-Filtered TEM. *J. Electron Microsc.* **2009**, *58*, 147–155.
28. Haider, M.; Hartel, P.; Müller, H.; Uhlemann, S.; Zach, J. Information Transfer in a TEM Corrected for Spherical and Chromatic Aberration. *Microsc. Microanal.* **2010**, *16*, 393–408.
29. Mukai, M.; Kaneyama, T.; Tomita, T.; Tsuno, K.; Terauchi, M.; Tsuda, K.; Naruse, M.; Honda, T.; Tanaka, M. Performance of a New Monochromator for a 200 kV Analytical Electron Microscope. *Microsc. Microanal.* **2005**, *11*, 944–945.

30. Warner, J. H.; Mukai, M.; Kirkland, A. I. Atomic Structure of ABC Rhombohedral Stacked Trilayer Graphene. *ACS Nano* **2012**, *6*, 5680–5686.
31. Robertson, A. W.; Allen, C. S.; Wu, Y. a; He, K.; Olivier, J.; Neethling, J.; Kirkland, A. I.; Warner, J. H. Spatial Control of Defect Creation in Graphene at the Nanoscale. *Nat. Commun.* **2012**, *3*, 1144.
32. Wu, Y. a; Fan, Y.; Speller, S.; Creeth, G. L.; Sadowski, J. T.; He, K.; Robertson, A. W.; Allen, C. S.; Warner, J. H. Large Single Crystals of Graphene on Melted Copper Using Chemical Vapor Deposition. *ACS Nano* **2012**, *6*, 5010–5017.
33. Ma, J.; Alfè, D.; Michaelides, A.; Wang, E. Stone-Wales Defects in Graphene and Other Planar sp2-Bonded Materials. *Phys. Rev. B* **2009**, *80*, 033407.
34. Robertson, A. W.; Montanari, B.; He, K.; Kim, J.; Allen, C. S.; Wu, Y. A.; Olivier, J.; Neethling, J.; Harrison, N.; Kirkland, A. I.; *et al.* Dynamics of Single Fe Atoms in Graphene Vacancies. *Nano Lett.* **2013**, *13*, 1468–1475.
35. Kotakoski, J.; Santos-Cottin, D.; Krasheninnikov, A. V. Stability of Graphene Edges under Electron Beam: Equilibrium Energetics *versus* Dynamic Effects. *ACS Nano* **2012**, *6*, 671–676.
36. Perdew, J. P.; Burke, K.; Ernzerhof, M. Generalized Gradient Approximation Made Simple. *Phys. Rev. Lett.* **1996**, *77*, 3865–3868.
37. Kresse, G.; Furthmu, J. Efficient Iterative Schemes for *ab Initio* Total-Energy Calculations Using a Plane-Wave Basis Set. *Phys. Rev. B* **1996**, *54*, 11169.